Localized domain wall nucleation dynamics in asymmetric ferromagnetic rings revealed by direct time-resolved magnetic imaging

Kornel Richter,[1] Andrea Krone,[1] Mohamad-Assaad Mawass,[1,2] Benjamin Krüger,[1] Markus Weigand,[2] Hermann Stoll,[2] Gisela Schütz,[2] and Mathias Kläui[1,3]

[1]*Institute of Physics, Johannes Gutenberg University Mainz, Staudinger Weg 7, 55128 Mainz, Germany*

[2]*Max Planck Institute for Intelligent Systems, Heisenbergstrasse 3, 70569 Stuttgart, Germany*

[3]*Graduate School of Excellence Materials Science in Mainz (MAINZ), Staudinger Weg 9, 55128 Mainz, Germany*

(Received 8 April 2016; revised manuscript received 27 June 2016; published 27 July 2016)

We report time-resolved observations of field-induced domain wall nucleation in asymmetric ferromagnetic rings using single direction field pulses and rotating fields. We show that the asymmetric geometry of a ring allows for controlling the position of nucleation events, when a domain wall is nucleated by a rotating magnetic field. Direct observation by scanning transmission x-ray microscopy (STXM) reveals that the nucleation of domain walls occurs through the creation of transient ripplelike structures. This magnetization state is found to exhibit a surprisingly high reproducibility even at room temperature and we determine the combinations of field strengths and field directions that allow for reliable nucleation of domain walls and directly quantify the stability of the magnetic states. Our analysis of the processes occurring during field induced domain wall nucleation shows how the effective fields determine the nucleation location reproducibly, which is a key prerequisite toward using domain walls for spintronic devices.

DOI: 10.1103/PhysRevB.94.024435

I. INTRODUCTION

Ferromagnetic rings are of particular interest due to their flux-closure state that is stray-field free and thus have a ground state configuration with particularly high stability [1,2]. This makes them a promising candidate for development of nonvolatile data storage devices with switching based on domain wall (DW) dynamics [3–6], where reproducible domain wall nucleation paves the way to reliable switching. However, to switch between the two possible vortex states used for data storage (clockwise and counterclockwise) directly, circular magnetic fields would be needed, which are difficult to generate [7]. A simpler and more accessible method is to switch with a homogeneous field from vortex state to the "onion state" with two domain walls [8] and then back to the vortex state with opposite chirality [8], which was also investigated theoretically in detail in Ref. [9]. For memory devices, it has been shown that magnetic rings down to sub-100-nm diameter show the two-step switching [10] that we investigate here, so that fundamentally the basic effect will also occur for smaller lateral sizes that are more relevant for highly integrated devices, while the devices for many sensors based on domain wall motion [11] are in the micrometer regime that we study here. General so far, these different switching processes occurring in rings have only been investigated in detail quasistatically [12]. And in particular the stability of the vortex state has not been quantified for the relevant ring geometries and the dynamics of switching from the vortex state including the key time scales is also largely unexplored.

First, the process of the switching from the onion to the vortex state occurs by domain wall motion and this has been studied in detail previously [7]. However, for the second step, the critical process of DW nucleation from the vortex state needed to switch to the onion state has not been investigated in real time and the dynamics have not been ascertained. In particular, as nucleation processes tend to depend on defects and thermal excitation that the reliability and reproducibility of these processes is not clear. Furthermore, this issue is compounded in simple symmetric rings, where demagnetizing fields do not depend on the applied field direction so that the nucleation position can be poorly defined. This leads to domain wall nucleation and propagation that is dependent on small variations in the local magnetic properties related to defects or edge roughness [13], leading to a large distribution of the nucleation fields. So in order to use devices with switching by domain wall nucleation, the dynamics needs to be understood and controlled and the stability of the vortex state needs to be determined.

In this paper we use tailored asymmetric ferromagnetic rings that introduce spatial variations to demagnetization fields and allow us to engineer the position of nucleation events that occur in particular positions of the ring. Our time-resolved observation of the nucleation process of domain walls reveals that the nucleation process runs through the creation of transient ripplelike structures characterized by periodically alternating magnetization directions. These previously neglected transient ripple patterns show a surprisingly high reproducibility and set the time scale of the nucleation process. Analyzing the relevant torques acting on the local magnetization reveals that the position of localized nucleation is not governed by a spatial distribution of local fluctuations of magnetic anisotropy, but the geometric shape of the sample allows us to engineer the nucleation event at a selected position of the ring. Finally, to ascertain the stability of the vortex state against external magnetic fields, we employ specially engineered rotating nucleation fields. We show that in such a setup, the stability of the vortex state is governed not only by the field strength but in particular by the relation between the sense of rotation of the applied field and the chirality of the initial vortex state, which has previously been neglected.

II. EXPERIMENT

Ferromagnetic $Ni_{80}Fe_{20}$ rings with an outer diameter of 5.5 μm, an inner diameter of 4 μm, and a thickness of 30 nm are

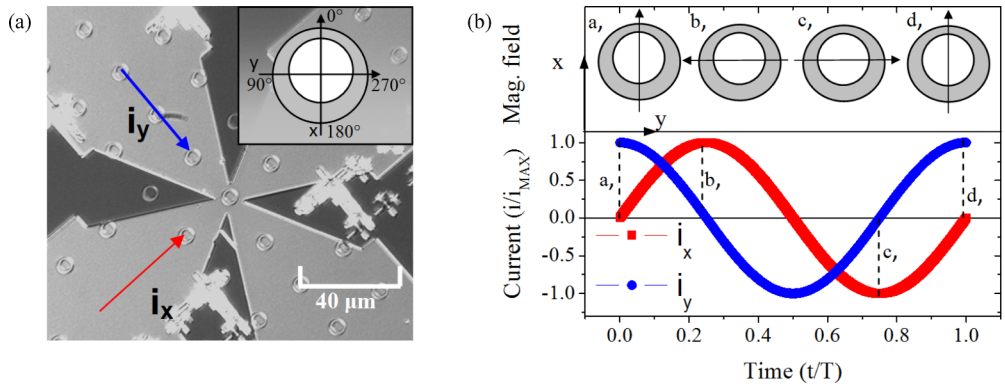

FIG. 1. (a) Optical image of the as-prepared sample containing asymmetric rings with 300 nm width in the narrowest part. The ring studied here is placed below the crossed striplines used to generate in-plane magnetic field. The inset shows the angle notation. (b) The rotating magnetic field is generated through sinusoidal currents with 90° phase shift in each of the striplines.

prepared by electron beam lithography and a lift-off process. In order to ascertain the influence of the ring asymmetry on the nucleation process, a series of asymmetric rings with different widths in the narrowest part are used, ranging from 100 to 500 nm in 100 nm steps. The field excitation is provided by a series of copper striplines deposited on top of the asymmetric ring [Fig. 1(a)] [14,15]. The two crossed striplines allow us to apply field pulses in any direction in the plane as well as rotating fields [Fig. 1(b)].

To analyze the reliability of the nucleation event and reproducibility of the ripple creation, we employ scanning transmission x-ray microscopy (STXM) [16] at the BESSY II synchrotron in Berlin. Besides having high temporal and spatial resolution, we additionally take advantage of the pump and probe scheme of this setup to determine the reliability. The samples are periodically excited by magnetic fields with more than 10^9 repetitions during the recording of a movie. Thus, the grayscale of resulting magnetic contrast naturally carries information on the reproducibility and reliability of dynamical processes, which is a key to studying the applicability for devices. X-ray magnetic circular dichroism (XMCD) is used as a contrast method to detect surface magnetization. This contrast mechanism is sensitive to the magnetization component parallel to the wave vector of incident light [17]. Since for in-plane magnetized samples and normal incidence of the circularly polarized light this component is zero, we tilt the whole setup vertically with respect to the beam by 30 deg. Thus, the resulting magnetic contrast is proportional to the horizontal component of magnetization.

III. RESULTS

We start by investigating domain wall nucleation dynamics using a uniform magnetic field pulse along a selected direction. This leads to a switching from the vortex to the onion state presented in Fig. 2. As seen, the whole switching event runs as a series of three successive magnetization processes. First, we see the (i) development of ripplelike magnetization pattern [see Fig. 2(b)], which is proceeded by the (ii) formation of two domain walls and reverse magnetization domain [Fig. 2(c)] followed by (iii) domain wall propagation towards the field direction in order to minimize the Zeeman energy [Figs. 2(d)–2(f)]. Therefore, the overall reproducibility of the switching process from the vortex to the onion state in given by reliability of all the involved processes.

The process of domain wall nucleation starts by the abrupt perturbation of the circular magnetization direction occurring at a position of approximately 30 deg [see $t = 4$ ns in Fig. 2(b)]. In this position the local magnetization spontaneously splits into small regions with alternating radial components of the magnetization, resulting in the appearance of transient ripplelike structures. Such metastable magnetization states have previously been studied statically or on slow time scales and are referred to as concertina pattern, or as an oscillatory buckling mode [18–20]. They consist of interacting low-angle Néel domain walls that stabilize their mutual distance by dipolar interactions [19]. A perpendicular orientation of ripples with respect to the average magnetization can be explained by smaller surface magnetic charges as compared to a longitudinal orientation. The appearance of magnetic ripples is sometimes expected to result from local magnetic anisotropy variations [21,22] characteristic for polycrystalline deposited thin films or resulting from edge roughness. However, micromagnetic simulations and theoretical calculations [19,21] show that metastable ripples can have a largely magnetostatic origin as well. As shown in Fig. 2(b), the spatial orientation of the ripples leads to enhanced periodicity for a smaller effective width of ring, which agrees with previous observations in wires with varying cross sections [23,24].

As seen in Fig. 2, the reproducibilities of the processes involved differ. Interestingly, the transient ripples magnetization pattern exhibits higher reproducibility than the formation of the domain walls. While the boundaries of ripples are well visible and separated [Fig. 2(b)], the spin dynamics during domain wall generation in Fig. 2(c) leads to a monotonous blurred contrast in the whole half-ring. Such poor reproducibility of the domain wall formation is then also responsible for fluctuations of the time at which both domain walls align with a field direction. This can be observed as the progressive increase of grayscale contrast of the vortex wall [Figs. 2(d)–2(f)], while the apparent position of domain wall does not change. As seen in Fig. 2, the development of ripples and their transformation to domain walls [Figs. 2(a)–2(d)] takes more than one half of the overall switching time (30 ns), thus governing the overall switching time [Fig. 2(c)]. Therefore, the initial stages of the

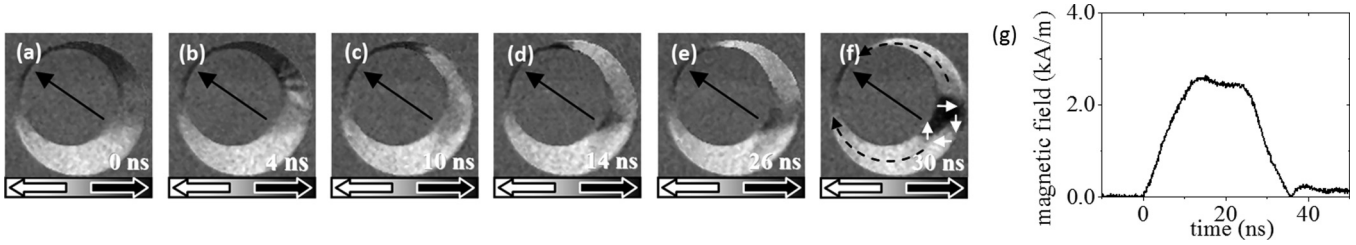

FIG. 2. (a)–(f) Switching from the vortex by the creation of the onion state by a pulse of a static magnetic field with an amplitude of 2.6 kA/m. The ferromagnetic ring with 100 nm width in the narrowest part is used for the experiment. The magnetization direction contrast is shown by arrows at the bottom. The magnetization direction in the domains (domain wall) is depicted by dashed arrows (white arrows) in (f). (g) The excitation process consists of applying a 37 ns long nucleation field pulse for the switching to the onion state. This is then followed by the switching back into the vortex state with the original chirality to enable a pump-probe measurement (not shown).

switching (development of ripples and formation of domain walls) are the most important factors that influence the overall reproducibility and time scales of the switching process from the vortex to the onion state.

Having established the dynamics of the wall nucleation, we next probe the stability of the vortex state. To this end we use magnetic fields in all directions, which is realized by a rotating magnetic field. Figures 3 and 4 compare the switching process from an initially CCW magnetized vortex state by using CW and CCW nucleating field rotation with the same field amplitude. For a CW rotating magnetic field [Fig. 3(a)], the process of domain wall creation runs through the asymmetric appearance of a ripplelike structure, similarly to Fig. 2(b) in the half-ring magnetized in the opposite direction with respect to the applied field. Magnetic ripples spread across a relatively large area of 4 μm in the energetically unfavorable half of the vortex state, until they reach the inner edge of the ring in the widest part [Figs. 3(b) and 3(c)]. The torque acting on the magnetic moments is at this position highest due to the higher curvature of the inner perimeter edge of the ring as compared to the outer one. Then, the magnetic ripples lead to the nucleation of the domain wall and a reverse magnetic domain (black magnetic contrast) that begins to spread. However, the domain wall never reaches the outer ring edge, and the reverse domain collapses again [Fig. 3(c)] into the original vortex state. The collapse of the reversed domain takes place by radial motion of domain wall towards the inner edge of the ring. By comparison of domain wall positions at $t = 30$ ns and $t = 38$ ns, the domain wall velocity can be estimated to around 40 m/s showing that domain walls can be displaced by the internal fields surprisingly rapidly. We see that due to the sense of field rotation and the initial vortex chirality, the rotating field as it continues to rotate does not stabilize the reverse domain. Thus the vortex state is particularly resistant against fields that rotate against the magnetization direction of its vortex state.

We now flip the rotation direction and rotate the field along the chirality of the CCW vortex state next. Figure 4 shows the nucleation event when the sense of the field rotation is the same as the (CCW) magnetization rotation of the initial vortex state. The nucleation event starts by a rapid development of magnetic ripples in the half-ring with magnetization oriented opposite to the field direction [i.e., around 160 deg position in Fig. 4(c)]. For this combination of magnetization and field rotation, the field amplitude is strong enough to lead to a fast growth of the reversed domain. In the middle of the onion state formation [Fig. 4(d)] there are one tail-to-tail domain wall aligned to the field direction and one head-to-head domain wall in the widest part of the ring. Further relaxation of the system leads to the onion state formation [Fig. 4(e)], where both domain walls propagate with a rotating magnetic field [Fig. 4(f)].

The observed behavior highlights that not only the amplitude and the frequency of rotating nucleation magnetic field, but a relation between sense of rotation of magnetic field and vortex chirality must be chosen judiciously in order to successfully switch from the vortex one to the onion state. This result has major implications for the design of magnetic devices employing rotating fields as for instance widely used in sensors [25], since the influence of the rotation field frequency on both domain wall dynamics and nucleation process must be taken into account.

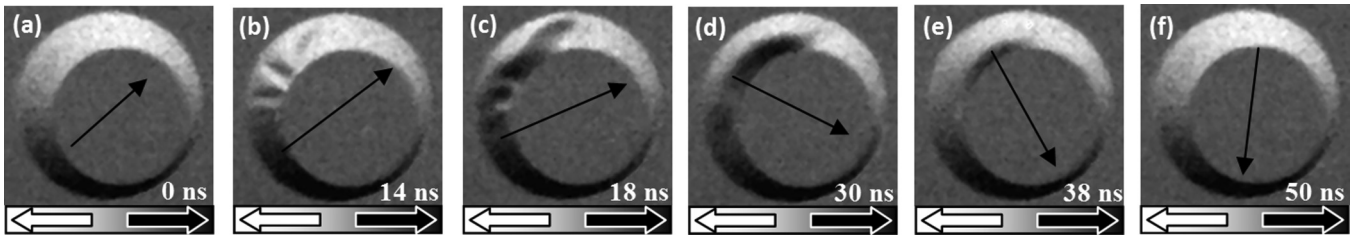

FIG. 3. Spin dynamics of the vortex state with CCW circulation driven by CW rotating magnetic field with an amplitude of 3.2 kA/m at 10 MHz frequency. A ferromagnetic ring with 300 nm width in the narrowest part is used for observation. (a) Initial vortex state of the magnetization configuration. (b) Ripples are formed preferably at the part of the ring that needs to change the magnetization direction during the switching. (c) DW nucleation and simultaneous reversal of part of the ring magnetization starting at the widest part from the inner edge of the ring structure.

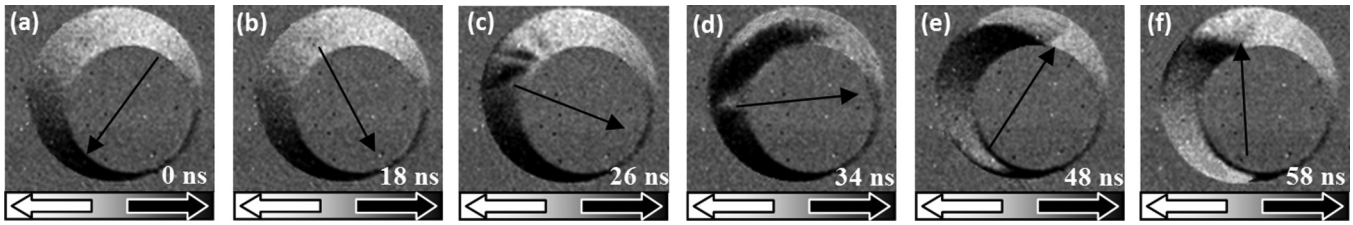

FIG. 4. Formation of the onion state by CCW field rotation. The ring is initially in vortex state with CCW magnetization. (a)–(d) Ripple formation and nucleation of domain walls. (e) and (f) The rotation of the walls after the onion state is nucleated. Observation is performed using ferromagnetic ring with 300 nm in the narrowest part. Excitation is done by magnetic field (depicted by black arrow) with the amplitude of 3.2 kA/m and 10 MHz frequency.

Finally, we analyze the nucleation event theoretically to understand the origin of the dynamics including in particular the position where it occurs. We examine the relevant magnetic torques acting on the local magnetization. If an external magnetic field H_{external} is applied to a ferromagnetic ring in the vortex state, the local magnetization M experiences a torque, which rotates the magnetization to align it with the local effective magnetic field:

$$\tau = -\gamma M \times (H_{\text{exch}} + H_{\text{stray}} + H_{\text{external}}) = -\gamma M \times H_{\text{eff}}. \tag{1}$$

Thus, the local torque acting on the magnetization depends on the strength of the local effective field (H_{eff}) and the angle of misalignment. For ferromagnetic rings in the vortex state, both vary as a function of the position. While the direction of the exchange and external fields are relatively straightforward, the stray fields are given by surface magnetic charges generated by magnetic moments misaligned from the circular direction parallel to the outer ring perimeter. Moreover, if a rotating field is used, the spatial distribution of the stray field is time dependent and due to the complex shape of ring structure, it cannot be estimated analytically. So to understand the role of asymmetric ring geometry [9] in the nucleation process, a series of micromagnetic simulations have been carried out to spatially resolve the effective field and the resulting torque.

Figure 5 compares time evolution of magnetization dynamics and relevant local effective magnetic fields during the nucleation process. At the beginning of the field rotation [Fig. 5(a) at $t = 20$ ns], the effective field is perpendicular to the local magnetization only along the field direction, which could lead to a largest torque at this position. However, the amplitude of the effective field is minimal there. Our analyses show that the position of highest torque in the vortex state is misaligned from the applied field direction and it is situated in the energetically unfavorable half-ring with opposite direction of magnetization with respect to the applied field [see black ellipses in Fig. 5(b)]. Thus, the maximum of torque in the system is not at the position of a 90 deg angle of misalignment, but dominated by the high amplitude of the effective field, which originates from the stray field that emerges from the particular shape of the sample and can thus be tuned by the shape.

As we have seen, the nucleation process of the onion state starts by the ripple formation and the consequent formation of two domain walls [$t = 31-37$ ns in Fig. 5(a)]. Residual domains with the magnetization aligned antiparallel [blue color in Fig. 5(a) at $t = 37$ ns] to the CCW magnetization

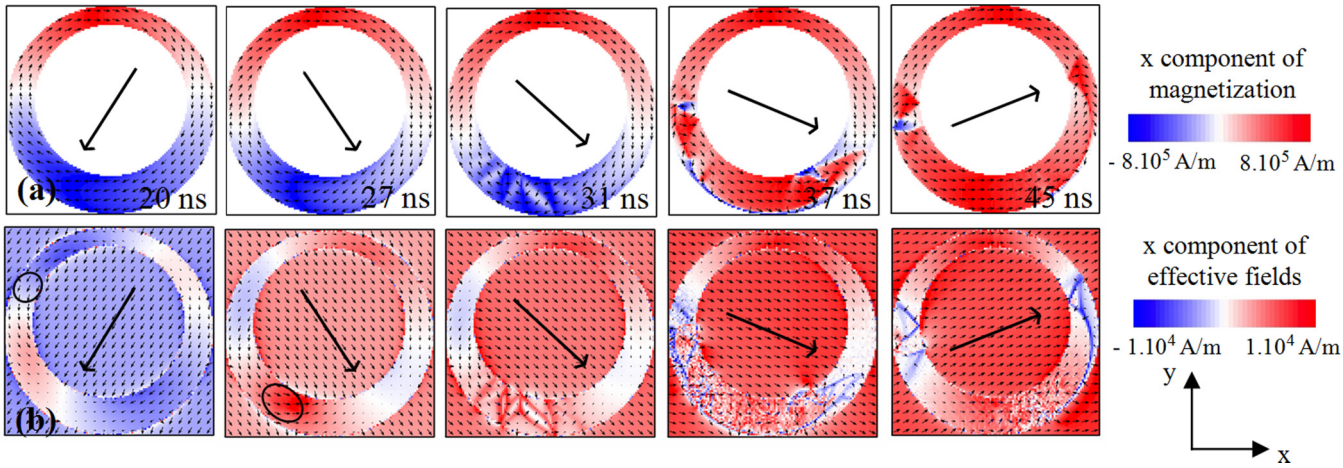

FIG. 5. Micromagnetic simulation of the domain wall nucleation by 10 MHz counterclockwise rotating magnetic field in an asymmetric ring with 500 nm width in the narrowest part. The amplitude of the nucleation field is 2 kA/m and the starting angle of the magnetic field is 90°. The orientation of the local fields is depicted by the direction of black arrows, while the field amplitude is imaged by the length of the arrows. (a) Time evolution of magnetization dynamics. (b) Snapshots of the effective field. The position of maximum torque is indicated by a black ellipse.

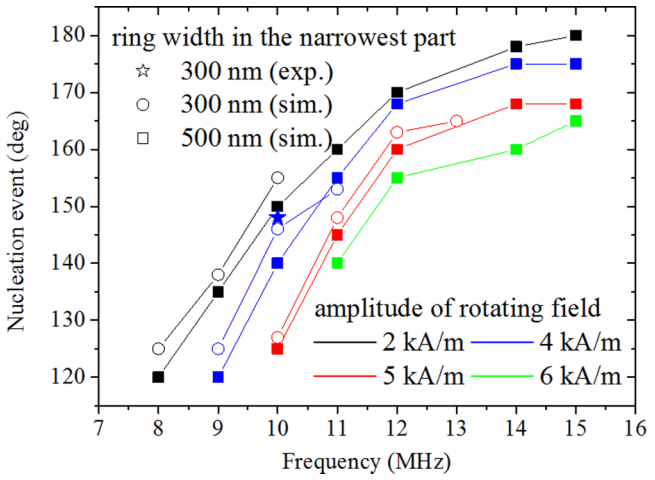

FIG. 6. Location of ripple creation as a function of CCW rotating field amplitude and ring asymmetry. Simulation and experimental data are obtained from the nucleation events originating from the rotating field. We use the angle definition from Fig. 1(a). The starting orientation of the nucleation field is 90°.

impede the formation of the onion state. These residual domains are then annihilated over 12 ns and the further evolution of the onion state formation is characterized by the relaxation of both domain walls towards the field direction. Thus, the development of magnetic ripples and the transformation into the stable domain wall structure takes more than 80% of total nucleation time and thus these previously neglected processes govern the time scale of the whole switching event. It is worth noting that even when changing the asymmetry of ferromagnetic rings, the ripple creation and development of domain wall spin structure take approximately the same time.

As noted above, the position of the ripple creation, and thus, the nucleation event is never aligned with an external field direction. Figure 6 systematically compares the position of ripple creation for several combinations of frequencies and amplitudes of field rotation. As seen, for a given frequency, the higher amplitude of the rotating field results in faster ripple creation after field excitation, and thus, the nucleation event occurs at lower angles. Changes of the position of ripple creation with varying frequency are however not very significant. The same behavior can be seen when varying the asymmetry of rings. For a smaller asymmetry of rings (i.e., the width in the narrowest part is larger), the position of nucleation event occurs at smaller angles. As noted above, the nucleation process of domain walls and the development of magnetization ripples is governed mostly by stray fields emanating from the curvature of the ring structure, so the effect of varying ring asymmetry on location of ripples creation is negligible as the curvature of structure is not changed significantly by changing the width of the narrower and wider part of the ring. The total nucleation time of the onion state is not strongly dependent on the ring asymmetry either, since the processes occurring during the nucleation are similar and both domain walls have to propagate along the same total distance (one half of a ring perimeter). Thus, the total nucleation time is mostly given by the amplitude of the driving field and not by the geometry at least within our probed range. So for potential applications requiring a localized nucleation with high spatial precision, this must be taken into account and by tuning the external field and the geometry the nucleation spots can be engineered.

IV. CONCLUSION

In conclusion, we determine the dynamics of the switching processes occurring associated with the nucleation of domain walls. We study in particular the vortex to the onion state switching in asymmetric ferromagnetic rings using unidirectional field pulses and rotating fields. Time-resolved observation of this switching from the vortex state to the onion state reveals that the process of domain wall nucleation runs through creation of a transient ripplelike magnetization pattern. Such a magnetization pattern is characterized by high reproducibility and long lifetime, thus governing the time of the overall switching process. By comparing different field sequences, we show that the vortex state is particularly resistant to a field that rotates against the magnetization direction of the initial vortex state. By analyzing the effective fields in micromagnetic simulations we show that the nucleation event occurs in the energetically unfavorable half-ring and its position is given by stray fields emerging from the sample shape. Our results show that the nucleation while being very reproducible depends in a complex fashion on the shape and details of the external field. This means that one needs to take into account all these factors to understand the switching, which however then allows one to actually engineer the switching dynamics. As curved geometries are widely used for instance in sensor devices based on domain our results represent a key step for the design of such future devices.

ACKNOWLEDGMENTS

This work is supported by the project Interfacing Oxides (IFOX) from the European Community's Seventh Framework Program (FP7/2007-2013) under grant agreement No. NMP3-LA-2010-246102, the Wall project (FP7-PEOPLE-2013-ITN 608031), Magwire FP7-ICT-2009-5 257707, MASPIC ERC-2007-StG 208162, MultiRev ERC-2014-PoC 665672, as well as the Center of Innovative and Emerging Materials at Johannes Gutenberg University Mainz, the Graduate School of Excellence Materials Science in Mainz (CSC 266) and the DFG (SFB TRR 173 Spin+X). B. Krüger acknowledges Carl Zeiss Stiftung. The authors gratefully acknowledge the beamline staff, Iuliia Bykova and Michael Bechtlel for the help with preparation and realization of the experiment and Jürgen Henrizi for the help with sample preparation.

[1] M. Saitoh, M. Kawabata, K. Harii, H. Miyajima, and T. Yamaoka, Manipulation of vortex circulation in decentered ferromagnetic nanorings, J. Appl. Phys. **95**, 1986 (2004).

[2] D. K. Singh, T. Yang, and M. T. Touminen, Magnetization vorticity and exchange bias phenomena in arrays of small asymmetric magnetic rings, Physica B **405**, 4377 (2015).

[3] J.-G. Zhu, Y. Zheng, and G. A. Prinz, Ultrahigh density vertical magnetoresistive random access memory, J. Appl. Phys. **87**, 6668 (2000).

[4] A. Imre, L. Zhou, A. Orlov, G. Csaba, G. H. Bernstein, W. Porod, and V. Metlushko, Application of mesoscopic magnetic rings for logic devices, *Fourth IEEE Conference on Nanotechnology, Munich, Germany* (IEEE, Piscataway, NJ, 2004), pp. 137–139.

[5] K. Richter, A. Krone, M.-A. Mawass, B. Krüger, M. Weigand, H. Stoll, G. Schütz, and M. Kläui, Local Domain Wall Velocity Engineering via Tailored Potential Landscapes in Ferromagnetic Rings, Phys. Rev. Appl. **5**, 024007 (2016).

[6] M. Curcic, H. Stoll, M. Weigand, V. Sackmann, P. Juellig, M. Kammerer, M. Noske, M. Sproll, B. Van Waeyenberge, A. Vansteenkiste, G. Woltersdorf, T. Tyliszczak, and G. Schütz, Magnetic vortex core reversal by rotating magnetic fields generated on micro-meter length scales, Phys. Status Solidi B **248**, 2317 (2011).

[7] M. Kläui, Head-to-head domain walls in magnetic nanostructures, J. Phys.: Condens. Matter **20**, 313001 (2008).

[8] J. Rothman, M. Kläui, L. Lopez-Diaz, C. A. F. Vaz, A. Bleloch, J. A. C. Bland, Z. Cui, and R. Speaks, Observation of a Bi-Domain State and Nucleation Free Switching in Mesoscopic Ring Magnets, Phys. Rev. Lett. **86**, 1098 (2001).

[9] S. Prosandeev, I. Ponomareva, I. Kornev, and L. Bellaiche, Control of Vortices by Homogeneous Fields in Asymmetric Ferroelectric and Ferromagnetic Rings, Phys. Rev. Lett. **100**, 047201 (2008).

[10] L. J. Heyderman, C. David, M. Kläui, C. A. F. Vaz, and J. A. C. Bland, Nanoscale ferromagnetic rings fabricated by electron-beam lithography, J. Appl. Phys. **93**, 10011 (2003).

[11] M. Diegel, M. Roland, and E. Halder, Multiturn counter using movement and storage of 180 magnetic domain walls, Sensor Lett. **5**, 118 (2007).

[12] M. Kläui, C. A. F. Vaz, L. Lopez-Diaz, and J. A. C. Bland, Vortex formation in narrow ferromagnetic rings, J. Phys.: Condens. Matter **15**, R985 (2003).

[13] J. Li, S. Zhang, Ch. Grigas, R. Misra, J. Bartell, V. H. Crespi, and P. Schiffer, Magnetization states and switching in narrow-gapped ferromagnetic nanorings, AIP Adv. **2**, 012136 (2012).

[14] A. Bisig, M. Stärk, M.-A. Mawass, Ch. Moutafis, J. Rhensius, J. Heidler, F. Büttner, M. Noske, M. Weigand, S. Eisebitt, T. Tyliszczak, B. Waeyenberge, H. Stoll, G. Schütz, and M. Kläui, Correlation between spin structure oscillations and domain wall velocities, Nat. Commun. **4**, 2328 (2013).

[15] M. Curcic, B. Van Waeyenberge, A. Vansteenkiste, M. Weigand, V. Sackmann, H. Stoll, M. Fähnle, T. Tyliszczak, G. Woltersdorf, C. H. Back, and G. Schütz, Polarisation Selective Magnetic Vortex Dynamics and Core Reversal in Rotating Magnetic Fields, Phys. Rev. Lett. **101**, 197204 (2008).

[16] D. Nolle, M. Weigand, P. Audeehm, E. Goering, U. Wiesemann, C. Wolter, E. Nolle, and G. Schütz, Note: Unique characterization possibilities in the ultrahigh vacuum scanning transmission x-ray microscope (UHV-STXM) "MAXYMUS" using a rotatable permanent magnetic field up to 0.22 T, Rev. Sci. Instrum. **83**, 046112 (2012).

[17] G. Schütz, W. Wagner, W. Wilhelm, P. Kienle, R. Zeller, R. Frahm, and G. Materlik, Absorption of Circularly Polarized x Rays in Iron, Phys. Rev. Lett. **58**, 737 (1987).

[18] H. A. M. van den Berg and D. K. Vatvani, Wall clusters in thin soft ferromagnetic configurations, J. Appl. Phys. **52**, 6830 (1981).

[19] R. Cantero-Alvarez and F. Otto, Oscillatory buckling mode in thin-film nucleation, J. Nonlinear Sci. **16**, 385 (2006).

[20] X. F. Han, M. Grimsditch, J. Meersschaut, A. Hoffmann, Y. Ji, J. Sort, J. Nogues, R. Divan, J. E. Pearson, and D. J. Keavney, Magnetic Instability Regions in Patterned Structures: Influence of Element Shape on Magnetization Reversal Dynamics, Phys. Rev. Lett. **98**, 147202 (2007).

[21] R. Cantero-Alvarez and F. Otto, Critical fields in ferromagnetic thin films: Identification of four regimes, J. Nonlinear Sci. **16**, 351 (2006).

[22] J. Steiner, R. Schäfer, H. Wieczoreck, J. McCord, and F. Otto, Formation and coarsening of the concertina magnetization pattern in elongated thin-film elements, Phys. Rev. B **85**, 104407 (2012).

[23] D. Chumakov, J. McCord, R. Schäfer, L. Schultz, H. Vinzelberg, R. Kaltofen, and I. Mönch, Nanosecond time-scale switching of permalloy thin film elements studied by wide-field time-resolved Kerr microscopy, Phys. Rev. B **71**, 014410 (2005).

[24] W. K. Hiebert, G. E. Ballentine, L. Lagae, R. W. Hunt, and M. R. Freeman, Ultrafast imaging of incoherent rotation magnetization switching with experimental and numerical micromagnetic dynamics, J. Appl. Phys. **92**, 392 (2002).

[25] M. Diegel, S. Glathe, R. Mattheis, M. Scherzinger, and E. Halder, A new four bit magnetic domain wall based multiturn counter, IEEE Trans. Magn. **45**, 3792 (2009).